DOI: 10.6060/mhc256412b

Synthesis and Evaluation of the Cytotoxicity of Zinc Porphyrinates Derived from Protoporphyrin IX Derivatives

Y. I. Pylina,[a] T. K. Rocheva,[b] I. S. Khudyaeva,[b] E. S. Belykh,[a] D. M. Shadrin,[a] N. D. Belykh,[c] and D. V. Belykh[b@]

[a]*Institute of Biology of Komi Scientific Center of the Ural Branch of the Russian Academy of Sciences, 167982 Syktyvkar, Russian Federation*
[b]*Institute of Chemistry of Komi Scientific Center of the Ural Branch of the Russian Academy of Sciences, 167982 Syktyvkar, Russian Federation*
[c]*Institute of Biology and Biomedicine, Lobachevsky State University, 603950 Nizhny Novgorod, Russian Federation*
[@]*Corresponding author E-mail: belykh-dv@chemi.komisc.ru, belykh-dv@mail.ru*

*New zinc complexes of protoporphyrin IX derivatives, specifically the dimethyl esters of deuteroporphyrin IX and mesoporphyrin (**1** and **2**), as well as their amide derivatives containing an ethanolamine fragment (**3** and **4**), were synthesized. The compounds obtained, with the exception of the **Zn-1** complex, exhibited low solubility, which precluded the evaluation of their dark cytotoxicity at concentrations exceeding 25 μM. The flow cytometry analysis demonstrated that ligands **1**, **3**, and **4**, along with the corresponding **Zn-1** to **Zn-4** complexes, were able to penetrate HeLa cells. The photoinduced cytotoxicity of the compounds studied was observed at concentrations lower than 1 μM. Fluorescence microscopy revealed that **Zn-1** molecules are localized both in mitochondria and the Golgi apparatus. Photoinduced exposure of **Zn-1** to HeLa cells resulted in an increase in reactive oxygen species levels and a decrease in mitochondrial membrane potential. Together with phosphatidylserine externalization, these results suggest a possible induction of regulated cell death after photoinduced exposure to **Zn-1**.*

Keywords: Protoporphyrin IX, zinc complexes, cytotoxicity, cellular uptake, ROS, mitochondrial potential.

Синтез и оценка цитотоксичности порфиринатов цинка на основе производных протопорфирина IX

Я. И. Пылина,[a] Т. К. Рочева,[b] И. С. Худяева,[b] Е. С. Белых,[a] Д. М. Шадрин,[a] Н. Д. Белых,[c] Д. В. Белых[b@]

[a]*Институт биологии Коми научного центра Уральского отделения Российской академии наук, 167982 Сыктывкар, Республика Коми, Россия*
[b]*Институт химии Коми научного центра Уральского отделения Российской академии наук, 167982 Сыктывкар, Республика Коми, Россия*
[c]*Институт биологии и биомедицины, Государственный университет имени Н.И. Лобачевского, 603950 Нижний Новгород, Россия*
[@]*E-mail: belykh-dv@chemi.komisc.ru, belykh-dv@mail.ru*

*Синтезированы новые комплексы цинка на основе производных протопорфирина IX, в частности диметиловых эфиров дейтеропорфирина IX и мезопорфирина IX (**1** и **2**), а также их амидных производных, содержащих фрагмент этаноламина (**3** и **4**). Полученные соединения, за исключением комплекса **Zn-1**, обладали низкой растворимостью, которая не позволила оценить их темновую цитотоксичность при концентрации больше 25 мкмоль/л. Методом проточной цитофлуориметрии установлено, что лиганды **1**, **3**, **4** и комплексы **Zn-1–4** на их основе проникают в клетки HeLa. Фотоиндуцированная цитотоксичность исследуемых соединений наблюдалась при концентрации ниже 1 мкМ. Методом флуоресцентной микроскопии показано, что **Zn-1** локализуется в митохондриях и аппарате Гольджи. Фотоиндуцированное воздействия **Zn-1** на клетки*

HeLa приводило к повышению уровня активных форм кислорода и снижению мембранного потенциала митохондрий. Вместе с экстернализацией фосфатидилсерина эти результаты свидетельствуют о возможной индукции регулируемой гибели клеток после фотоиндуцированного воздействия ***Zn-1****.*

Ключевые слова: Протопорфирин IX, комплексы цинка, цитотоксичность, клеточное поглощение, активные формы кислорода, потенциал митохондрий.

Introduction

Natural and synthetic porphyrins are known to accumulate in malignant neoplasms, a property that, along with their ability to generate singlet oxygen upon light exposure, is widely used in photodynamic therapy for oncological diseases.[1-6] Derivatives of protoporphyrin IX are employed in clinical practice; therefore, new macro-heterocyclic compounds obtained through chemical modification of protoporphyrin IX can be considered potential antitumor photosensitizers (PS).[7-13] The structural similarity between the products of chemical modification of hemin and its derivatives and endogenous porphyrins raises hopes for their relatively low toxicity. Metalloporphyrins also hold promise for biomedical applications: the introduction of a metal ion can enhance the physicochemical properties of the compound compared to the ligand, suggesting the potential use of metallo-porphyrins in medical diagnostics as tumor imaging agents.[2,4,14] Furthermore, metal porphyrinates are used for pathogen destruction,[15-16] with zinc-porphyrin complexes demonstrating the highest efficacy against protozoa and bacteria. The potential shift of the absorption maximum toward the orange region of the spectrum, compared to the ligand, facilitates the use of photoinduction by sunlight.

The introduction of a metal ion can enhance the photodynamic properties of the compound.[17-19] In particular, it has been demonstrated that incorporating a zinc ion into the coordination sphere of the porphyrin increases the photoinduced cytotoxicity of the compound compared to the ligand. This enhancement is likely attributed to increased interactions with cell membranes, which may result from the ability of zinc porphyrinates to form additional complexes with the phosphate groups of phospholipids.[18] Furthermore, the potential release of a zinc ion during the photodecomposition of the complex may amplify the antitumor effect; it is known that several zinc complexes are considered promising candidates for antitumor drugs, with their efficacy in some cases linked to alterations in zinc concentration within tumor cells.[20-24] Among zinc complexes of tetrapyrrole compounds, complexes of phthalocyanines and tetra-*meso*-arylporphyrins have been investigated as photoindependent antitumor agents and photosensitizers.[24] In contrast, similar complexes based on blood porphyrins as potential antitumor agents have not been described in the literature. Therefore, the synthesis of new zinc complexes derived from protoporphyrin IX derivatives and the investigation of their biological properties as potential photosensitizers (PS) is of significant interest. In this study, new zinc porphyrinates based on dimethyl esters of deuteroporphyrin IX and mesoporphyrin IX, along with their diamide derivatives containing an ethanolamine fragment, were synthesized, and their dark and photoinduced cytotoxicity was evaluated.

Experimental

General

IR spectra were recorded in KBr tablets on a Shimadzu IR Prestige 21 device. UV–vis spectra were recorded on a Shimadzu UV-1700 spectrometer with the wavelength range of 250–900 nm. The samples were analyzed in quartz cuvettes (10 mm thick). ^{1}H NMR spectra of the synthesized compounds were recorded on a Bruker AVANCE-II-300 spectrometer using standard impulse Bruker software. The chemical shift values are expressed as δ ppm down field with residual protons of the solvent (DMSO-d_6: δ 2.50 ppm, $CDCl_3$ 7.26 ppm) as internal standard. The assignment of signals in the spectra of the obtained compounds was carried out using the results of two-dimensional experiments (NOESY, COSY). Mass spectra (ESI) were recorded on a Thermo-Finnigan LCQ Fleet device. The reaction was controlled using TLC method on Sorbfil slides. Extraction of the reaction products was done using column chromatography on silica gel Alfa Aesar, 70–230 mesh. Hemin (AppliChem, Germany, was used for protoporphyrin IX derivatives obtaining).

Synthesis

Synthesis and spectral characteristics of protoporphyrin IX derivatives (**1-4**) are presented in our earlier work.[25]

Zn(II)-2,7,12,18-Tetramethyl-13,17-di(2′-carbomethoxy)-ethylporphine ***(Zn-1)****.* A solution of $Zn(CH_3COO)_2$ (46 mg, 0.251 mmol) in 3 mL of methanol was added to a solution of porphyrin **1** (15 mg, 0.028 mmol) in 4 mL of chloroform. The reaction mixture was kept at room temperature for 24 h, then diluted with chloroform (30 mL) and the organic phase was washed with water to remove methanol and excess zinc acetate. The resulting solution was dried with anhydrous Na_2SO_4, the solvent was removed under reduced pressure. 11 mg (64 % yield) of the target product **(Zn-1)** was obtained as a red-brown powder. MS (ESI), *m/z* (relative intensity of peak in cluster, %) for $[MH]^+$: $^{12}C_{32}H_{33}N_4O_4{}^{64}Zn$ found 601.3 (100 %), calculated 601.2 (100 %); $^{13}C_{32}H_{33}N_4O_4{}^{64}Zn$ found 602.4 (53 %), calculated 602.2 (37 %), $^{12}C_{32}H_{33}N_4O_4{}^{66}Zn$ found 603.6 (77 %), calculated 603.2 (65 %); $^{13}C_{32}H_{33}N_4O_4{}^{66}Zn$ found 604.4 (50 %), calculated 604.2 (31 %), $^{12}C_{32}H_{33}N_4O_4{}^{68}Zn$ found 605.4 (61 %), calculated 605.2 (46 %); for $[MNa]^+$: $^{12}C_{32}H_{32}N_4NaO_4{}^{64}Zn$ found 623.3 (100 %), calculated 623.2 (100 %); $^{13}C_{32}H_{32}N_4NaO_4{}^{64}Zn$ found 624.3 (41 %), calculated 624.2 (37 %), $^{12}C_{32}H_{32}N_4NaO_4{}^{66}Zn$ found 625.6 (65 %), calculated 625.2 (65 %); $^{13}C_{32}H_{32}N_4NaO_4{}^{66}Zn$ found 626.3 (35 %), calculated 626.2 (31 %), $^{12}C_{32}H_{32}N_4NaO_4{}^{68}Zn$ found 627.2 (35 %), calculated 627.2 (46 %), $^{13}C_{32}H_{32}N_4NaO_4{}^{68}Zn$ found 628.0 (23 %), calculated 628.2 (15 %). IR (KBr) ν cm^{-1}: 2955, 2914, 2857 (CH_3, CH_2), 1732 ($\nu_{C=O}$, ester), 1568, 1441, 1364, 1287, 1203, 1177, 974, 841, 750. UV-Vis ($CHCl_3$) λ_{max} nm (I_{rel}, %): 568.0 (6), 533.5 (7), 402.5 (100). ^{1}H NMR ($CDCl_3$) δ ppm (*J*, Hz): 3.30–3.33 (m, 4H, 13-CH_2CH_2COOCH$_3$, 17-CH_2CH_2COOCH$_3$), 3.60, 3.61, 3.62, 3.66 (all s 3H, 2-CH_3, 7-CH_3, 12-CH_3, 18-CH_3), 3.73, 3.76 (all s 3H, 13-CH_2CH_2COOCH_3, 17-CH_2CH_2COOCH_3), 4.40 (t, 4H, 13-CH_2CH$_2$COOCH$_3$, 17-CH_2CH$_2$COOCH$_3$, *J* = 6.8), 9.22, 9.24 (all s 1H, 3-H, 8-H), 10.11, 10.13, 10.14, 10.18 (all s 1H, 5-H, 10-H, 15-H, 20-H).

Zn(II)-2,7,12,18-Tetramethyl-3,8-diethyl-13,17-di(2′-carbomethoxy)ethylporphine ***(Zn-2)***. A solution of $Zn(CH_3COO)_2$ (46 mg, 0.251 mmol) in 3 mL of methanol was added to a solution of porphyrin **2** (15 mg, 0.028 mmol) in 4 mL of chloroform. The reaction mixture was kept at room temperature for 24 h, then diluted with chloroform (30 mL) and the organic phase was washed with water to remove methanol and excess zinc acetate. The resulting solution was dried with anhydrous Na_2SO_4, the solvent was removed under reduced pressure. 10 mg (59 % yield) of the target product **(Zn-2)** was obtained as a red-brown powder. MS (ESI), *m/z* (relative intensity of peak in cluster, %) for $[MNa]^+$: $^{12}C_{36}H_{40}N_4NaO_4{}^{64}Zn$ found 679.7 (100 %), calculated 679.2 (100 %); $^{13}C_{36}H_{40}N_4NaO_4{}^{64}Zn$ found 680.7 (54 %), calculated 680.2 (41 %), $^{12}C_{36}H_{40}N_4NaO_4{}^{66}Zn$ found 681.7 (58 %), calculated 681.2 (66 %); $^{13}C_{36}H_{40}N_4NaO_4{}^{66}Zn$ found 682.6 (36 %), calculated 682.2 (33 %), $^{12}C_{36}H_{40}N_4NaO_4{}^{68}Zn$ found 683.7 (45 %), calculated 683.2 (47 %), $^{13}C_{36}H_{40}N_4NaO_4{}^{68}Zn$ found 684.8 (24 %), calculated 684.2 (17 %). IR (KBr) ν cm^{-1}: 2959, 2924, 2859 (CH_3, CH_2), 1734 ($\nu_{C=O}$, ester), 1543, 1441, 1377, 1258, 1142, 988, 835, 714. UV-Vis (C_2H_5OH) λ_{max} nm (I_{rel}, %): 569.5 (10), 532.5 (8), 402.0 (100). ^{1}H NMR ($CDCl_3$) δ ppm (*J*, Hz): 1.77–1.86 (m, 6H, 3-CH_2CH_3, 8-CH_2CH_3), 3.17–3.24 (m, 4 H, 13-CH_2CH_2COO, 17-CH_2CH_2COO), 3.48, 3.52, 3.53, 3.58, 3.69, 3.72 (all s 3H, 2-CH_3, 7-CH_3, 12-CH_3, 18-CH_3, 13-$CH_2CH_2COOCH_3$, 17-$CH_2CH_2COOCH_3$), 3.89–4.02 (m, 4H, 3-CH_2CH_3, 8-CH_2CH_3), 4.24–4.35 (m, 4H, 13-CH_2CH_2COO, 17-CH_2CH_2COO), 9.63, 9.64, 9.68, 9.75 (all s 1H, 5-H, 10-H, 15-H, 20-H).

Zn(II)-2,7,12,18-Tetramethyl-13,17-di[2′-N-(2-hydroxyethyl)-carbamoyl]ethylporphine ***(Zn-3)***. A solution of $Zn(CH_3COO)_2$ (46 mg, 0.251 mmol) in 3 mL of methanol was added to a solution of porphyrin **3** (14 mg, 0.023 mmol) in a mixture of 7 mL of chloroform and 9 mL of methanol (dissolution on heating). The reaction mixture was kept at room temperature for 24 h, then the solution was diluted with water (50 mL), and the resulting precipitate was filtered, washed with water and dried in air. 10 mg (67 % yield) of the target product **(Zn-3)** was obtained as a red-brown powder. MS (ESI), *m/z* (relative intensity of peak in cluster, %) for $[MH]^+$: $^{12}C_{34}H_{39}N_6O_4{}^{64}Zn$ found 659.3 (100 %), calculated 659.2 (100 %); $^{13}C_{34}H_{39}N_6O_4{}^{64}Zn$ found 660.4 (39 %), calculated 660.2 (40 %), $^{12}C_{34}H_{39}N_6O_4{}^{66}Zn$ found 661.3 (58 %), calculated 661.2 (66 %); $^{13}C_{34}H_{39}N_6O_4{}^{66}Zn$ found 662.3 (29 %), calculated 662.2 (32 %); $^{12}C_{34}H_{39}N_6O_4{}^{68}Zn$ found 663.3 (44 %), calculated 663.2 (47 %), $^{13}C_{34}H_{39}N_6O_4{}^{68}Zn$ found 664.4 (19 %), calculated 664,2 (17 %). IR (KBr) ν cm^{-1}: 3088 ($\nu_{N—H}$, $NHCH_2CH_2OH$), 2922, 2859 (CH_3, CH_2), 1639 ($\nu_{C=O}$, amid I), 1553, 1456, 1373, 1271, 1063, 970, 843, 750. UV-Vis (C_2H_5OH) λ_{max} nm (I_{rel}, %): 572.5 (4), 536.5 (5), 406.0 (100). ^{1}H NMR (DMSO-d_6) δ ppm (*J*, Hz): 3.06–3.21 (m, 8H, 13-CH_2CH_2CONHCH$_2$CH_2OH, 17-CH_2CH_2CONHCH$_2$CH_2OH), 3.32–3.34 (m, 4H, 13-CH_2CH_2CONHCH_2CH$_2$OH, 17-CH_2CH_2CONHCH_2CH$_2$OH), 3.61, 3.65, 3.72, 3.76 (all s 3H, 2-CH_3, 7-CH_3, 12-CH_3, 18-CH_3), 4.34 (t, 4H, 13-CH_2CH_2CONHCH$_2$CH$_2$OH, 17-CH_2CH_2CONHCH$_2$CH$_2$OH, *J* = 7.2), 4.61 (t, 2H, HNCH$_2$CH$_2$O*H*, *J* = 5.1), 8.10 (t, 2 H, *H*NCH$_2$CH$_2$OH, *J* = 5.3), 9.22, 9.23 (all s, 1H, 3-H, 8-H), 10.09, 10.13, 10.16, 10.21 (all s 1H, 5-H, 10-H, 15-H, 20-H).

Zn(II)-2,7,12,18-Tetramethyl-3,8-diethyl-13,17-di[2′-N-(2-hydroxyethyl)carbamoyl]ethylporphine ***(Zn-4)***. A solution of $Zn(CH_3COO)_2$ (46 mg, 0.251 mmol) in 4 mL of methanol was added to a solution of porphyrin **4** (16 mg, 0.025 mmol) in a mixture of 4 mL of chloroform and 4 mL of methanol (dissolution at heating). The reaction mixture was kept at room temperature for 24 h, then the solution was diluted with water (50 mL), and the resulting precipitate was filtered, washed with water and dried in air. 14 mg (80 % yield) of the target product **(Zn-4)** was obtained as a red-brown powder. MS (ESI), *m/z* (relative intensity of peak in cluster, %) for $[MH]^+$: $^{12}C_{38}H_{47}N_6O_4{}^{64}Zn$ found 715.4 (100 %), calculated 715.3 (100 %); $^{13}C_{38}H_{47}N_6O_4{}^{64}Zn$ found 716.45 (46 %), calculated 716.3 (44 %), $^{12}C_{38}H_{47}N_6O_4{}^{66}Zn$ found 717.4 (67 %), calculated 717.3 (68 %); $^{13}C_{38}H_{47}N_6O_4{}^{66}Zn$ found 718.5 (37 %), calculated 718.3 (35 %), $^{12}C_{38}H_{47}N_6O_4{}^{68}Zn$ found 719.4 (53 %), calculated 719.3 (48 %), $^{13}C_{38}H_{47}N_6O_4{}^{68}Zn$ found 720.5 (21 %), calculated 720.3 (19 %). IR (KBr) ν cm^{-1}: 3092 ($\nu_{N—H}$, $NHCH_2CH_2OH$), 2961, 2928, 2866 (CH_3, CH_2), 1643 ($\nu_{C=O}$, amid I), 1551, 1456, 1381, 1269, 1144, 989, 837, 710. UV-Vis (C_2H_5OH) λ_{max} nm (I_{rel}, %): 575 (7), 538.5 (8), 407.5 (100). ^{1}H NMR (DMSO-d_6) δ ppm (*J*, Hz): 1.85 (t, 6H, 3-CH_2CH_3, 8-CH_2CH_3, *J* = 6.7), 3.02–3.20 (m, 8H, 13-CH_2CH_2CONHCH$_2$CH_2OH, 17-CH_2CH_2CONHCH$_2$CH_2OH), 3.32–3.34 (m, 4H, 13-NHCH_2CH$_2$OH, 17-NHCH_2CH$_2$OH), 3.63 (all s 3H, 2-CH_3, 7-CH_3, 12-CH_3, 18-CH_3), 4.06–4.11 (m, 4H, 3-CH_2CH_3, 8-CH_2CH_3), 4.36 (t, 4H, 13-CH_2CH_2CONHCH$_2$CH$_2$OH, 17-CH_2CH_2CONHCH$_2$CH$_2$OH, *J* = 7.2), 4.61 (t, 2H, NHCH$_2$CH$_2$O*H*, *J* = 5.1), 8.10 (t, 2H, N*H*CH$_2$CH$_2$OH, *J* = 5.3), 10.07, 10.09, 10.18, 10.20 (all s 1H, 5-H, 10-H, 15-H, 20-H).

Biological research

Cell cultures. Human cervical carcinoma HeLa cells, human lung adenocarcinoma A549 cells, and human embryonic lung fibroblasts (HELF-104) (BioloT, Russia) were used. The cells were cultured in DMEM/F12 nutrient medium (PanEco, Russia) supplemented with 10% fetal bovine serum (FBS) (Beijing, China) and 1% L-glutamine (PanEco, Russia), without the addition of antibiotics, at 37 °C in a humidified atmosphere containing 5% CO_2. Cells were reseeded using a 0.05% trypsin-EDTA solution with Hanks' salts (PanEco, Russia) twice a week.

Dark cytotoxicity was estimated by a fluorimetric microculture cytotoxic assay (FMCA).[26] Stock solutions of compounds were prepared in DMSO (Amresco, USA) at a concentration of 20 mM. Working solutions were prepared by diluting the stock solution in DMSO. A volume of 1 μL of the appropriate compound solution was added to 199 μL of the nutrient medium containing 5000 HeLa or A549 cells and 1000 HELF-104 cells per well of a sterile 96-well culture plate. The final concentrations of compounds ranged from 0.015 to 100 μM, with the DMSO concentration maintained at 0.5% (v/v) in all experiments. Cells with added DMSO were used as a control. The cells were incubated for 72 h at 37 °C, 100% humidity, in an atmosphere containing 5% CO_2. Following incubation, the cells were washed with PBS (PanEco, Russia), and 100 μL of fluorescein diacetate solution (Sigma, USA) was added before incubation for an additional 40 minutes. Fluorescence intensity was then measured using a CLARIOstar microplate reader (BMG LABTECH, Germany) at wavelengths of 485 nm/520 nm. Cell survival was calculated as the ratio of the fluorescence intensity of the cells exposed to the compound to that of the control cells, expressed as a percentage.

Photoinduced cytotoxicity was assessed by the FMCA method similar to the determination of dark cytotoxicity. Two hours after incubation of the cells with the compound at the appropriate concentrations, they were illuminated for 20 min with cold daylight (for these and subsequent photoinduction experiments, an Osram L36W/756 lamp was used, the light dose 8 J/cm^2). The cells were then incubated in the dark for 70 h at 37 °C, 100% humidity in an atmosphere containing 5% CO_2.

ROS assessment in the cell culture was performed using the H2DCFDA reagent (2′,7′-dichlorodihydrofluorescein diacetate) (Lumiprobe, Russia) on a flow cytometer (Beckman Coulter, USA). HeLa cells (100,000 cells/mL) were seeded in a 12-well plate. After 24 h, the nutrient medium was replaced with fresh medium containing the compound at concentrations of 0.25 and 0.5 μM (added as a solution in DMSO) or with DMSO along. The cells were incubated for 2 h and illuminated for 20 min to photoinduce ROS, and then incubated for another 40 min in the dark. Control samples were incubated in the dark. Then the nutrient medium was removed, the cells were washed with 1xPBS, trypsinized, and a working solution of H2DCFDA dye at a concentration of 25 μM was added and incubated for 30 min. Fluorescence intensity was measured on a Cytoflex flow cytometer (Beckman Coulter, USA) (488 nm / 525 nm).

Compound uptake by cells. HeLa cells (100.000 cells/mL) were seeded in Petri dishes (∅ 60 mm). After 24 h, the nutrient medium was replaced with fresh medium containing the studied compounds at a concentration of 1 μM. The cells were then incubated in the dark for 10, 30, 120 min, and 24 h. Following incubation, the nutrient medium was removed, and the cells were washed twice with 1x PBS solution, trypsinized, and analyzed for fluorescence intensity (405 nm/610 nm) using a Cytoflex flow cytometer (Beckman Coulter, USA).

Intracellular localization of the compound. HeLa cells (100,000 cells/mL) were seeded in the 8-well cell culture slide (SPL Lifesciences, Korea). After 24 hours, the nutrient medium was replaced with fresh medium containing the studied compounds at a concentration of 0.25 μM. After one hour of incubation, the cells were stained according to the dye manufacturer's instructions and visualized using a fluorescence microscope (Biolam-L, LOMO, Russia). The dyes used included LumiTracker® Mito Rhodamine 123 (Lumiprobe, Russia), LumiTracker® Lyso Green (Lumiprobe, Russia), BDP® FL ceramide (Lumiprobe, Russia), and Hoechst 33258 (Sigma, USA). Images were captured using an camera MC-12 (LOMO, Russia) with a 20× objective lens.

Annexin V:FITC and Propidium Iodide (PI) differential staining analysis. HeLa cells (100,000 cells/mL) were seeded in a 12-well plate overnight. After 24 h, the nutrient medium was replaced with fresh medium containing the **Zn-1** compound at concentrations of 0, 0.25, and 0.5 μM. The cells were incubated for 2 h and then illuminated for 20 minutes. Control samples were incubated in the dark. After an additional 40 min, the cells were stained with Annexin V-FITC and PI (Wuhan Servicebio Technology Co., Ltd., China) according to the manufacturer's instructions. Fluorescence intensity was measured at 525 nm for Annexin V-FITC and at 585 nm for PI using a flow cytometer (Beckman Coulter, USA).

Analysis of mitochondrial membrane potential. HeLa cells (100,000 cells/mL) were seeded in a 12-well plate overnight. After 24 hours, the nutrient medium was replaced with fresh medium containing the **Zn-1** compound at concentrations of 0, 0.25, and 0.5 μM. The cells were incubated for 2 h and then illuminated for 20 min. Control samples were incubated in the dark. After an additional 40 min, the cells were stained using the JC-1 Mitochondrial Membrane Potential Assay Kit (Wuhan Servicebio Technology Co., Ltd., China) according to the manufacturer's protocol. To assess changes in mitochondrial membrane potential, the ratio of fluorescence intensity measured at 610 nm to that measured at 525 nm was determined using a flow cytometer (Beckman Coulter, USA). HeLa cells incubated with carbonyl cyanide 3-chlorophenylhydrazone (CCCP) at a concentration of 150 μM for 40 minutes served as a positive control.

Statistical analysis. The experimental results are presented as mean values ± standard deviation. For cell survival analysis, each data point represents the mean of at least six independent replicates. Samples were assessed for artifacts using Grubbs' test. The half-maximal growth inhibitory concentration (IC_{50}), defined as the concentration at which 50% of cells survive after 72 h of incubation with the substance, was calculated using the drc package in the R programming environment.[27] Analyses of ROS, Annexin V-FITC and PI staining, and mitochondrial membrane potential were performed in three independent experiments for each experimental variant. Statistical analysis of the results was performed using R software.[28] Data were tested for normality using the Shapiro-Wilk test. Multiple pairwise comparisons were conducted using either the Tukey test or Dunn's test at a significance level of 95%.

Results and Discussion

Synthesis and compounds' properties

As noted above, derivatives of deuteroporphyrin IX and mesoporphyrin IX (dimethyl esters **1** and **2**, and diamide derivatives with ethanolamine fragments **3** and **4**, as shown in Figure 1), which were synthesized from hemin using our previously developed methods, were selected for the study of dark and photoinduced cytotoxicity.[25] The synthesis of **Zn-1-4** complexes was performed by treating the initial ligands with zinc acetate in a mixture of chloroform and methanol. The structures of the obtained complexes were established based on data from electronic (UV-Vis), IR, and ^{1}H NMR spectroscopy, as well as mass spectrometry. In the UV-Vis spectra of the obtained complexes, changes characteristic of complex formation are observed compared to the spectra of the initial ligands, including a decrease in the number of bands in the visible region and a shift toward shorter wavelengths. The ^{1}H NMR spectra of the obtained compounds show signals corresponding to protons of substituents in the macrocycle that are

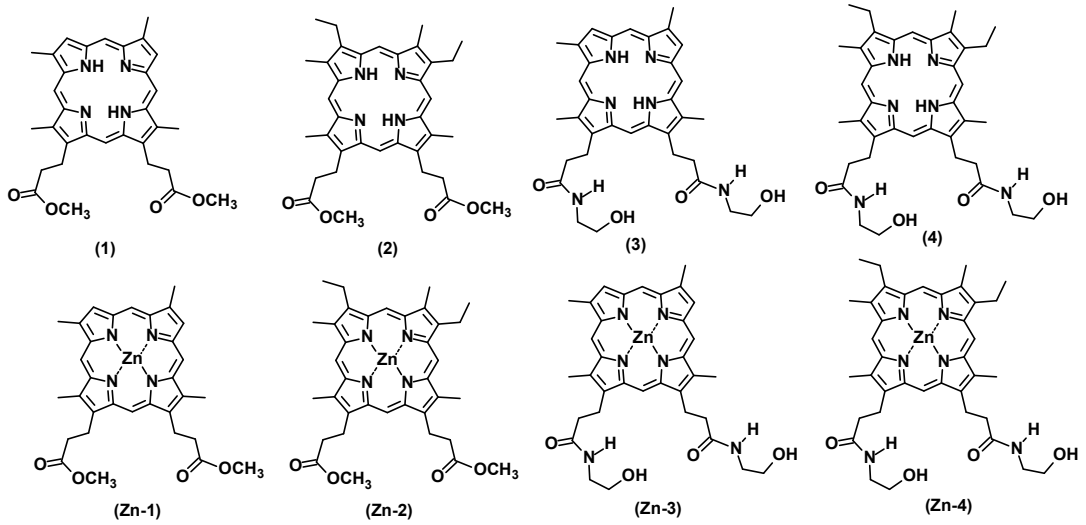

Figure 1. Structures of ligands (dimethyl esters **1** and **2**, and diamide derivatives with ethanolamine fragments **3** and **4)** and corresponding Zn complexes.

Table 1. IC_{50} values for dark and photoinduced cytotoxicity of compounds studied on cells of HeLa, A549 and HELF-104 cell lines.

Compound	IC_{50dark}, μM	$IC_{50photo}$, μM
	HeLa	
1	>6.25	0.0222±0.0002
Zn-1	>100	0.067±0.004
2*	No data	No data
Zn-2	>12.5	0.135±0.016
3	>3.12	0.108±0.006
Zn-3	>3.12	0.288±0.006
4	>3.12	0.061±0.002
Zn-4	>25	0.499±0.026
	A549	
1	>6.25	0.036±0.001
Zn-1	>100	0.094±0.001
	HELF-104	
1	>6.25	0.062±0.013
Zn-1	>100	0.183±0.063

Note: * - the compound was insoluble in DMSO.

similar to those of the corresponding initial ligands, indicating the preservation of peripheral substituents within the macrocycle. Notably, the ^{1}H NMR spectra do not exhibit signals from intracyclic NH protons that would be substituted by a zinc cation. In the mass spectra of the obtained compounds, peaks are observed with *m/z* values corresponding to protonated molecular ions of the complexes; the isotopic distribution in these clusters aligns with the presence of a zinc atom.

In the present study, dark and photoinduced cytotoxicity were assessed using the protocol described by Lindhagen *et al.*[26] and its modified version by Pylina *et al.*,[29] in which the compound under investigation is added to the cell suspension as a DMSO solution. The amount of DMSO added alongside the compound corresponds to a 0.5 % concentration in the culture medium. Such concentrations of DMSO do not exert a noticeable toxic effect on cells. It is important to note that the water solubility of the compound under investigation is not required when using this protocol.[30-31] We have successfully employed this method to study the dark and photoinduced cytotoxicity of a large set of chlorophyll *a* derivatives, most of which are insoluble in water.[29,32-33] When a water-insoluble compound is introduced into the cell medium from a DMSO solution, a dispersed system forms as a result of the interaction between the introduced compound and the components of the cell medium. Depending on its solubility in water, this interaction can range from single molecules to large aggregates or colloidal particles stabilized by components of the cell medium. The compound, which presents in the resulting dispersed system, regardless of its solubility in water, penetrates the cells and exerts a biological effect. However, if the introduced compound does not dissolve in water and interacts relatively weakly with cell components, a coarse solid phase may form, which can be detected using microscopy. Compounds contained within large particles are likely much less accessible or completely inaccessible for absorption by cells. Therefore, the formation of a coarse solid phase establishes an upper limit on the concentrations of a given compound available for study. It should be noted that low solubility in water or even its complete absence is not an obstacle to the use of the compound as a medical PS: the use of various solubilizers allows for the necessary bioavailability of porphyrin PS,[34-40] including protoporphyrin derivatives.[34]

It was found that the formation of dispersed systems with compounds accessible for absorption by cells, in the case of protoporphyrin derivatives, is feasible not for the entire range of concentrations (typically up to 100 μM; for example,[41-44]), which are used to assess the cytotoxicity of chlorin and porphyrin PS. Table 1 presents the upper limit of the concentrations of the studied compounds for which dark cytotoxicity can be evaluated.

Given the relatively narrow concentration range of the obtained compounds suitable for cytotoxicity studies, their uptake by cells was preliminarily examined using flow cytometry. Both the complexes and the corresponding ligands (with the exception of DMSO-insoluble ligand **2**) were shown to penetrate into the cells. As illustrated in Figure 2, fluorescence intensity was higher in cells cultured in the presence of the compounds under investigation compared to intact cells.

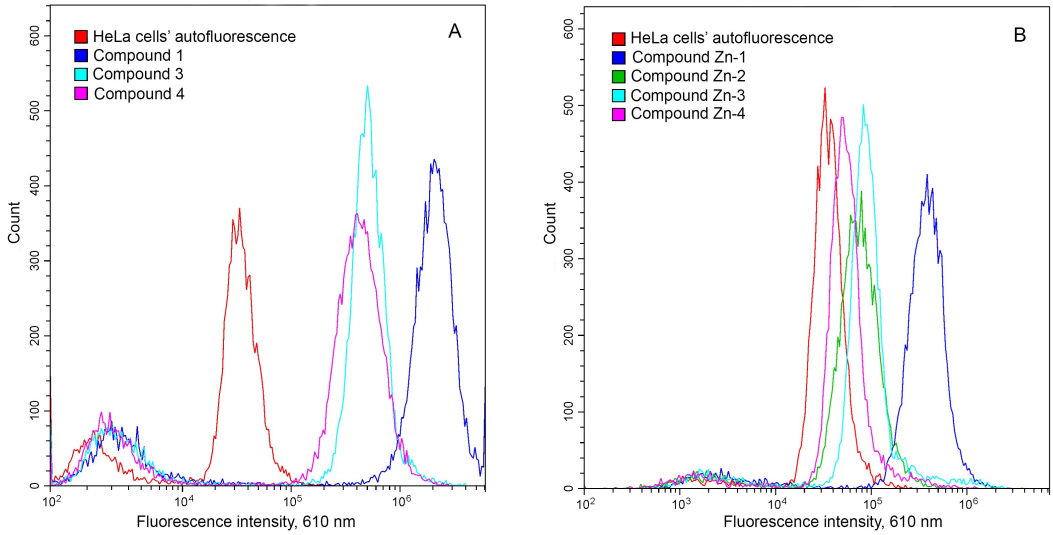

Figure 2. Absorption of the ligands **1**, **3**, **4** (A) and the corresponding complexes **Zn-1**-**4** (B) in HeLa cells assessed with the flow cytometry at 405 nm / 610 nm after two hours incubation at 1 μM.

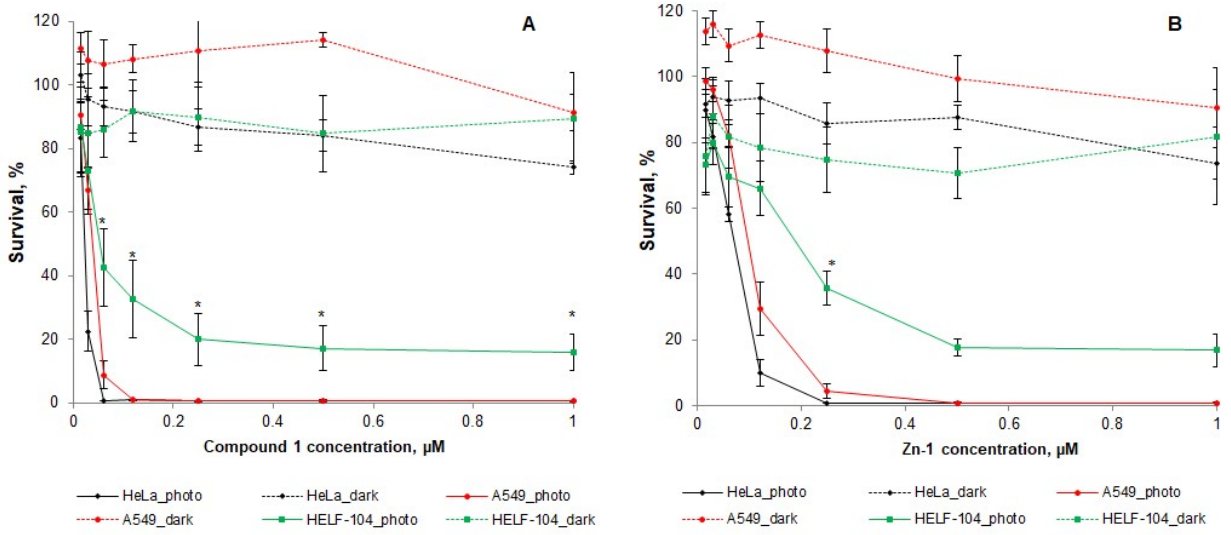

Figure 3. The survival of cells from HeLa, A549 and HELF-104 lines after compounds **1** (A) and **Zn-1** (B) dark and photoinduced exposure. * - differences in HeLa and A549 cells from the corresponded values for HELF-104 cells are significant at $p<0.05$ (Dunn test).

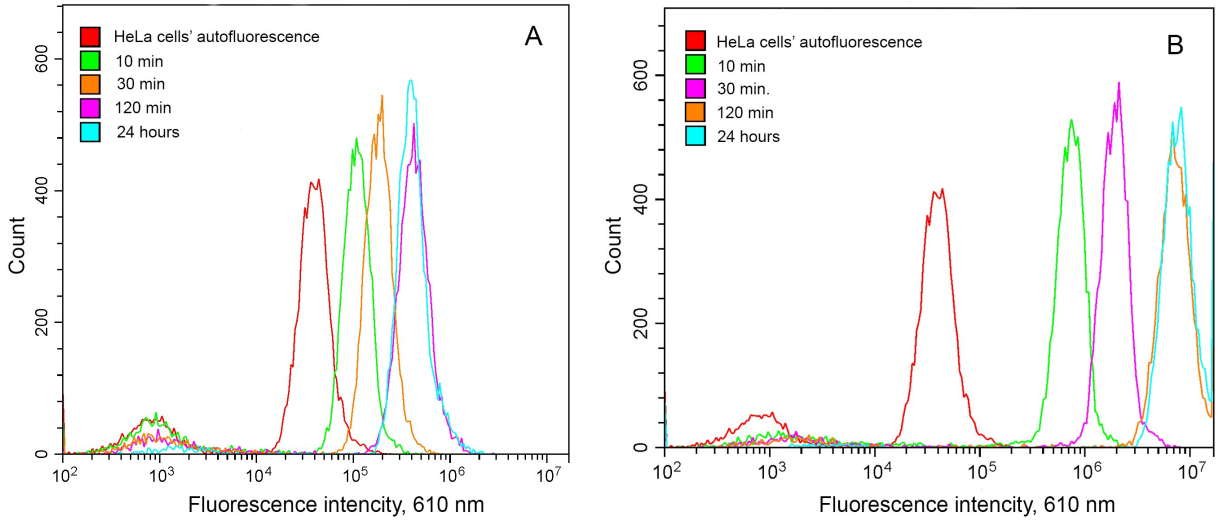

Figure 4. Flow cytometry assessment of compounds **Zn-1** (A) and **1** (B) fluorescence in HeLa cells after 10, 30, 120 min or, 24 hours addition (1 μM) into suspension at 405 nm / 610 nm.

Study of cytotoxicity of compounds

Evaluation of dark and photoinduced cytotoxicity of ligands and corresponding zinc complexes. Dark cytotoxicity was assessed using a fluorimetric microculture cytotoxicity assay (FMCA),[26] with photoinduced cytotoxicity determined according to the method described by Pylina *et al.*[29] Due to the weak absorption of the studied compounds in the red region, a light source with spectral characteristics similar to daylight was employed. Based on a large number of chlorophyll a derivatives for which IC_{50} values for dark cytotoxicity (IC_{50dark}) were determined according to the protocols used, cytotoxicity when comparing ligand-complex pairs. **Zn-1** is an exception: when this complex is introduced into the cell medium at a concentration of 100 μM, no formation of large solid particles occurs, and a decrease in cell survival to 73.7 ± 5.0% is observed, indicating a weak cytotoxic effect (Table 1). Thus, the IC_{50dark} for **Zn-1** is greater than 100 μM, classifying it as a compound with low cytotoxicity.

The $IC_{50photo}$ values for all studied compounds fall within the concentration ranges available for study, enabling an assessment of the effect of zinc cation incorporation on photoinduced cytotoxicity by comparing $IC_{50photo}$ values in ligand-complex pairs. In all cases, the photoinduced cytotoxicity of the complexes is lower than that of the corresponding ligands. For the ligand – **Zn-1** pair and ligand – **Zn-3** pair, the $IC_{50photo}$ differs by approximately threefold; in contrast, for the ligand – **Zn-4** pair, the $IC_{50photo}$ differs by more than eightfold. It should be noted that cytotoxicity of zinc porphyrinates based on tetra-*meso*-arylporphyrins has been reported to increase or remain unchanged compared to that of their corresponding ligands.[15,16,45] The data presented above indicate that among the studied compounds, the **Zn-1** complex is the most promising potential candidate for antitumor PS. This

complex not only exhibits the highest photoinduced cytotoxicity among all the investigated complexes but also surpasses or is comparable to the ligands examined in this study in this regard. Furthermore, the **Zn-1** complex demonstrates low dark cytotoxicity and does not form a coarse solid phase detectable by microscopy. Consequently, the biological properties of the ligand **1** and **Zn-1** complex pair were studied in greater detail. Studies of compounds **1** and **Zn-1** on another malignant human cell line A549 demonstrate a decrease in the photoinduced cytotoxicity of the **Zn-1** complex compared to ligand **1** (Figure 3, Table 1). A similar decrease in the photoinduced cytotoxicity of compound **Zn-1** compared to compound **1** is also observed when these compounds are tested on normal human embryonic fibroblasts (HELF-104 cell line) (Figure 3, Table 1). Furthermore, it is noteworthy that photocytotoxicity of the studied compounds is significantly lower in normal cells compared to malignant cell lines.

*Subcellular distribution and absorption of compounds **1**, **3**, **4** and **Zn-1**-**Zn-4**.* To assess the absorption of compounds **1** and **Zn-1**, fluorescence intensity in HeLa cells was measured at 10, 30, and 120 min, and 24 h. It was found that at a concentration of 1 μM for both compounds in the cell medium, fluorescence intensity reaches a maximum two hours after the introduction of the substance and remains at the same level for up to 24 h. The presence of a zinc cation in the coordination sphere of porphyrin does not appear to affect the rate of accumulation of the compound in cells (Figure 4).

The subcellular localization of the compounds was investigated by staining with specific organelle markers. Image analysis (Figures 5-6, Supp. 1) revealed that compounds **1**, **3**, and **4** predominantly accumulated in the mitochondria. Additionally, the localization of compound **3** in the Golgi apparatus was observed. For the Zn-complexes, localization was noted not only in the mitochondria but also in the Golgi apparatus for **Zn-1** and **Zn-2**, and in lysosomes for **Zn-4**. In contrast, **Zn-3** exhibited localization exclusively in the mitochondria, as indicated by the coincidence with organelle markers. Localization in the nucleus was not revealed for all the protoporphyrin IX derivatives studied. Changes in the localization of compounds may be one of possible causes of the decreased cytotoxicity of Zn complexes compared to corresponding ligands.

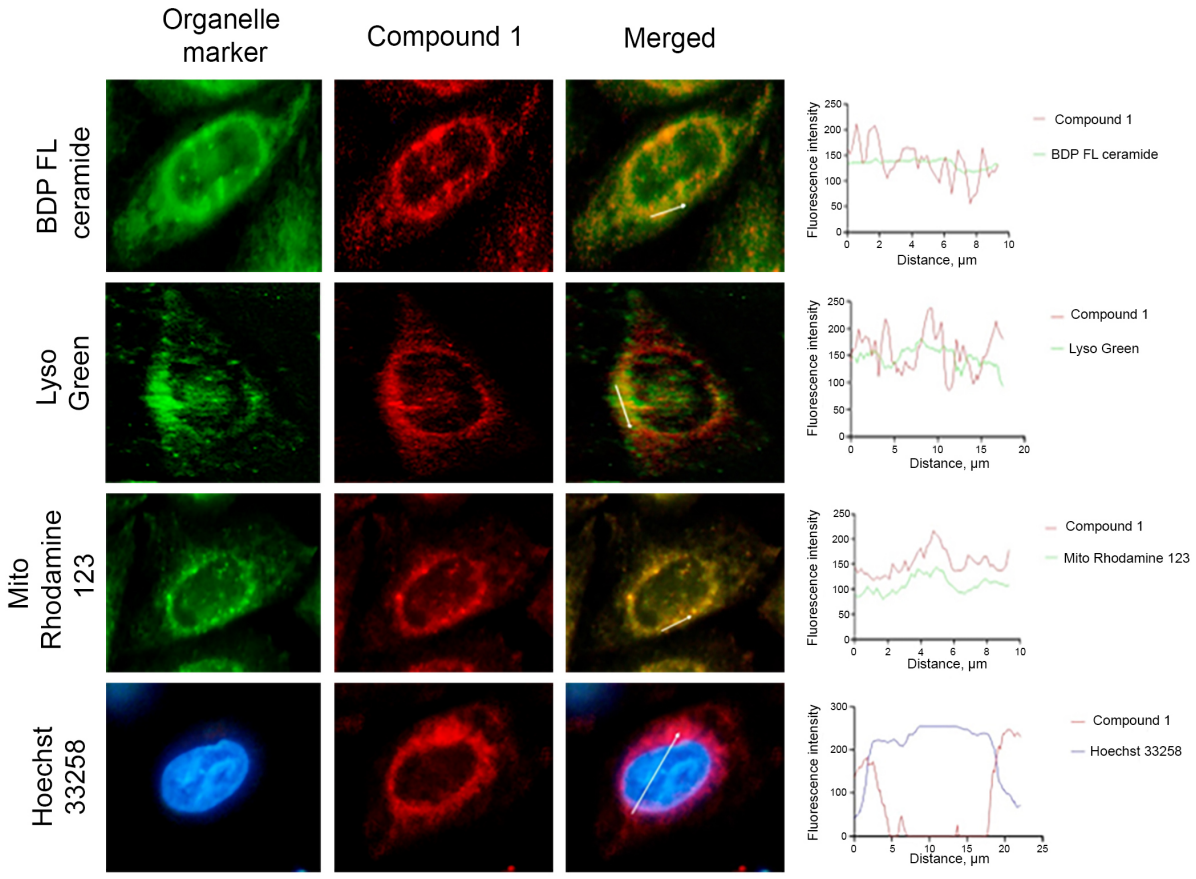

Figure 5. The subcellular localization of the compound **1** in HeLa cells. The following dyes were used: BDP® FL ceramide for Golgi apparatus, LumiTracker® Lyso Green for lysosomes, LumiTracker® Mito Rhodamine 123 for mitochondria and Hoechst 33258 for nuclei. In graphs: red line – fluorescence intensity of photosensitizer; green or blue line – fluorescence intensity of dye in the indicated cellular compartment (Ifl, a.u. ×103). Scale bars, 20 μm.

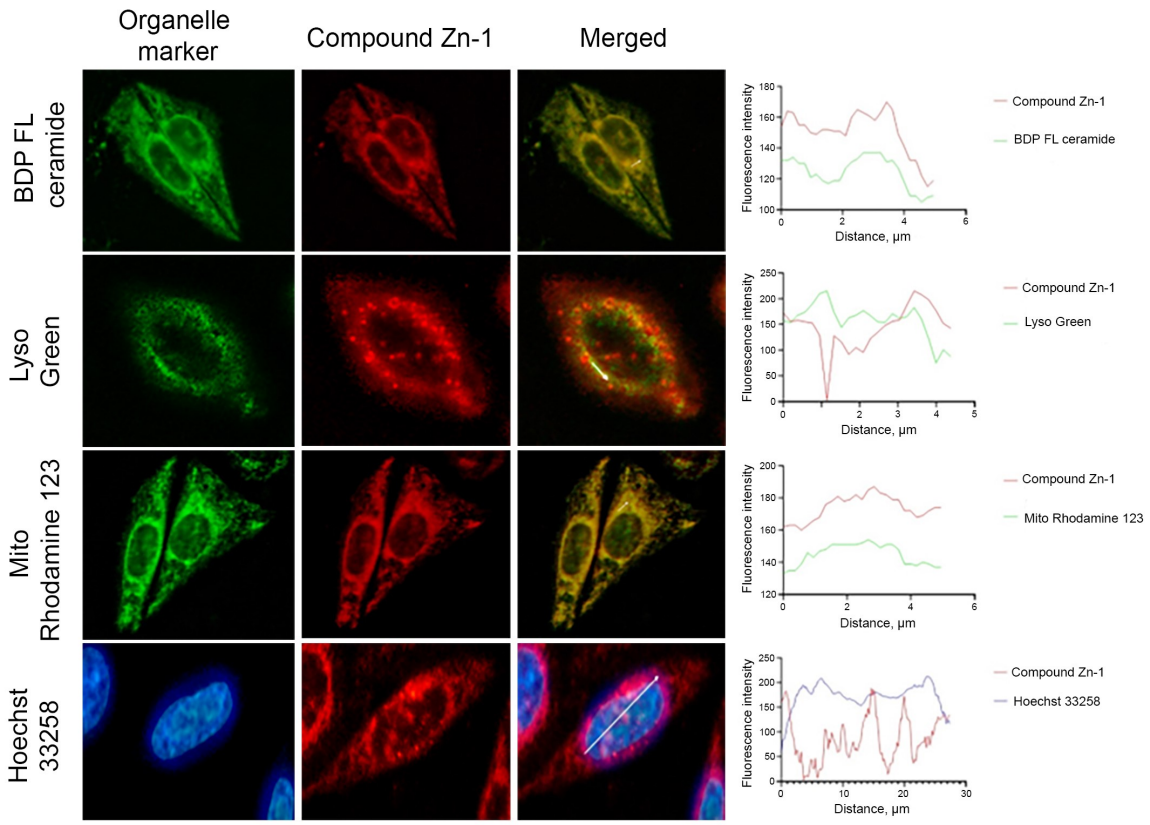

Figure 6. The subcellular localization of the compound **Zn-1** in HeLa cells. The following dyes were used: BDP® FL ceramide for Golgi apparatus, LumiTracker® Lyso Green for lysosomes, LumiTracker® Mito Rhodamine 123 for mitochondria and Hoechst 33258 for nuclei. In graphs: red line – fluorescence intensity of photosensitizer; green or blue line – fluorescence intensity of dye in the indicated cellular compartment (Ifl, a.u. ×103). Scale bars, 20 μm.

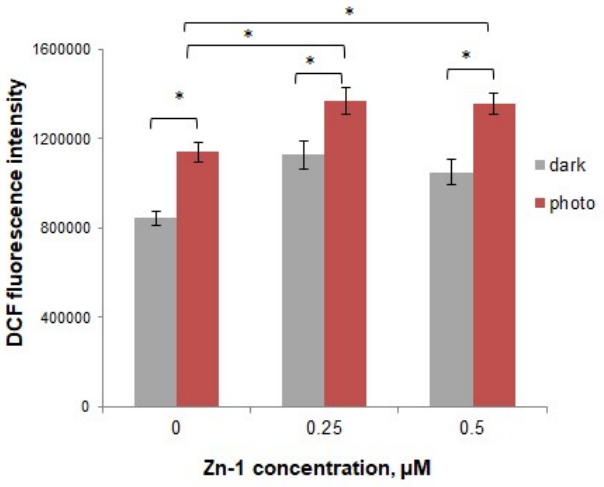

Figure 7. DCF fluorescence intensity in HeLa cells 40 min after photoinduced exposure of the **Zn-1** (0 - DMSO 0.5% v/v only), 0.25 and 0.5 μM. * - significantly different at $p<0.05$ (Tukey test).

*Effect of photoinduced exposure to the **Zn-1** compound on intracellular ROS levels.* An increase in intracellular ROS levels can play a significant role in triggering various types of regulated cell death, including paraptosis, apoptosis, ferroptosis, necroptosis, and autophagy.[46-48] It was found that after photoinduced exposure to the **Zn-1** compound at concentrations of 0.25 and 0.5 μM, there was a statistically significant increase in the fluorescence intensity of DCF in HeLa cells compared to the control group, indicating an elevation in ROS content following irradiation (Figure 7).

*Assessment of the phosphatidylserine externalization after **Zn-1** photoinduced exposure.* Differential staining with Annexin V-FITC and propidium iodide (PI) enables the assessment of phosphatidylserine, a marker of regulated cell death, on the surface of cell membranes,[49-50] while simultaneously evaluating the proportion of cells that have died as a result of membrane damage. In the absence of **Zn-1**, as well as in the case of dark exposure of the compound, the proportion of cells labeled with Annexin V or PI did not exceed 5% (Figure 8). However, 40 minu after photo-induced exposure to **Zn-1**, an increase in the proportion of stained cells was observed. Notably, the lower concentration studied resulted in a significant increase only in the proportion of cells stained with Annexin V (up to 5.85%). In contrast, at the higher concentration, there was an increase in the proportion of cells labeled with Annexin V (up to 37.60%), as well as a significant number of dead cells, marked with PI (up to 18.25%). Thus, the photo-induced exposure of **Zn-1** compound at low concentrations induces the appearance of phosphatidylserine on the cell surface, while at higher concentrations it leads to membrane damage also. This observed effect indicating the low intrinsic cytotoxicity of **Zn-1**.

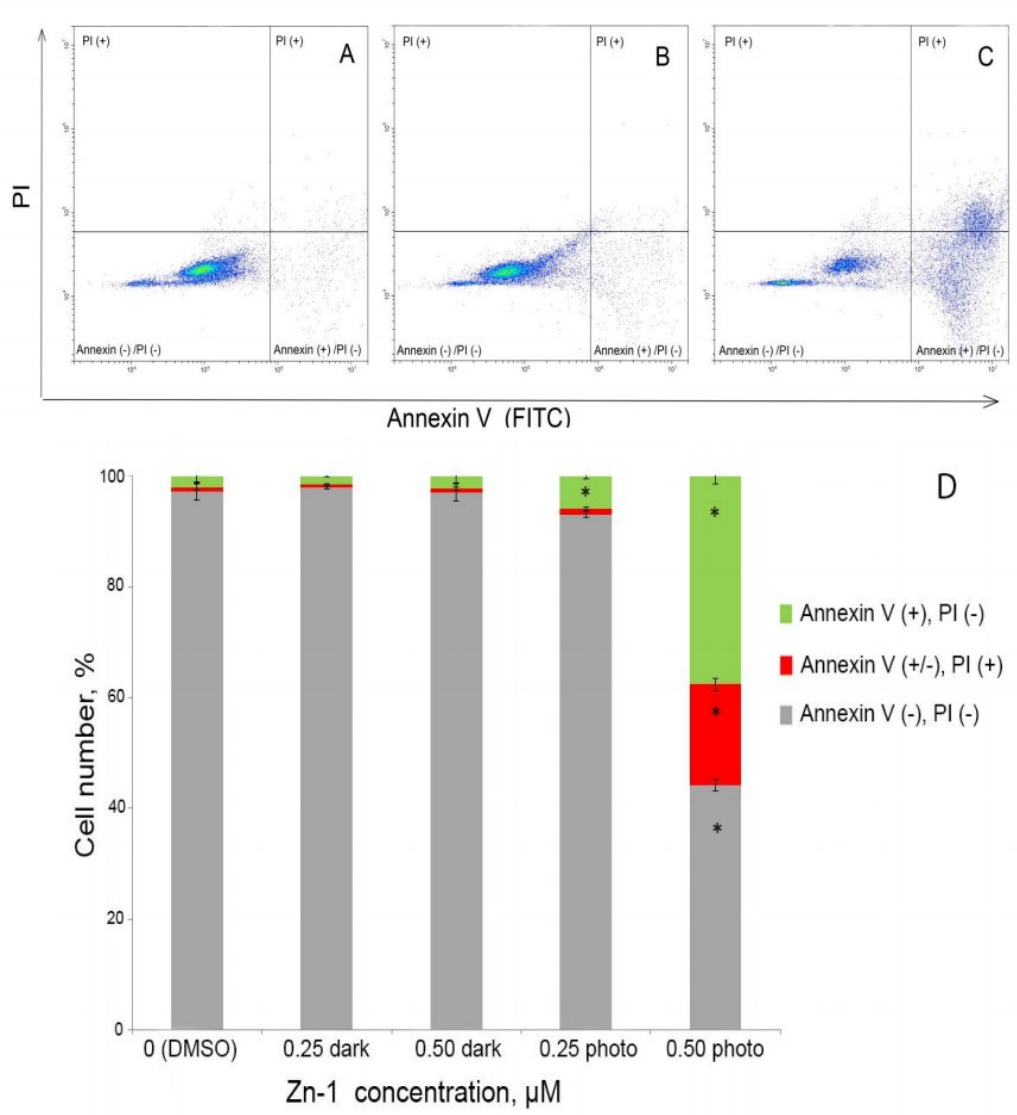

Figure 8. Distribution of HeLa cells into live («PI-AnnV-»), early apoptotic («PI-AnnV+»), and dead («AnnV+/-PI+») after **Zn-1** photo exposure in 0 (A), 0.25 (B) and 0.5 (C) μM. D – part of cells stained with Annexin-V-FITC and PI after **Zn-1** dark and light exposure. * - significantly different at $p < 0.05$ (Dunn test).

*Effect of photoinduced exposure of the **Zn-1** compound on the mitochondrial membrane potential of HeLa cells.*

Since the **Zn-1** compound was found to be localized in mitochondria, it is likely that these organelles are targets of its photoinduced action. Therefore, we assessed the mitochondrial membrane potential of HeLa cells after exposure to the **Zn-1** compound at concentrations of 0.25 and 0.5 μM using staining with the fluorescent dye JC-1. Flow cytometry analysis revealed that the photoinduced exposure of the **Zn-1** compound at a concentration of 0.5 μM resulted in a decrease in mitochondrial membrane potential (Figure 9) compared to the same concentration of **Zn-1** in the absence of irradiation, as well as after irradiation of cells in the presence of only the solvent (DMSO). The observed decrease in mitochondrial membrane potential, along with the appearance of phosphatidylserine on the cell surface, may indicate the induction of regulated cell death.[51-54]

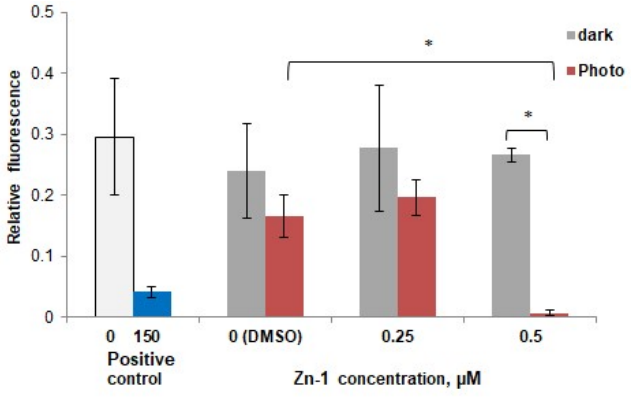

Figure 9. Mitochondrial membrane potential assessed with JC-1 in HeLa cells exposed to **Zn-1** (0, 0.25 and 0.5 μM).
* - significantly different at $p < 0.05$ (Tukey test). Carbonyl cyanide 3-chlorophenylhydrazone (150 μM, 40 min) used as a positive control.

Conclusions

We have synthesized new zinc porphyrinates based on protoporphyrin IX derivatives, namely the dimethyl esters of deuteroporphyrin IX and mesoporphyrin IX, as well as their amide derivatives containing an ethanolamine fragment. The low bioavailability of these compounds in the test system used precluded the evaluation of their dark cytotoxicity (with the exception of compound **Zn-1**); however, the photoinduced effects of these compounds were observed at significantly lower concentrations (less than 1 μM). For the most promising compound, **Zn-1**, it was demonstrated that the trends in photoinduced cytotoxicity upon transitioning from the metal-free porphyrin **1** to the **Zn-1** complex are preserved not only for malignant cell lines A549 and HeLa but also for non-immortalized HELF-104 cells. Notably, the photoinduced cytotoxicity of **Zn-1** was found to be higher in the A549 and HeLa cell lines compared to HELF-104. Furthermore, it was found that the **Zn-1** complex localizes in the mitochondria and Golgi apparatus of HeLa cells, generates intracellular ROS under light exposure, and likely induces a regulated type of cell death, mediated by mitochondrial damage and accompanied by disruption of plasma membrane integrity. Thus, **Zn-1** is of significant interest for further investigation as a potential antitumor PS for photodynamic therapy in oncological diseases.

Acknowledgements. The compounds synthesized were analyzed using the equipment of the Center of Collective Usage «Chemistry» at the Institute of Chemistry of the Komi Scientific Centre of the Ural Branch RAS. The studies of biological activity were carried out using the equipment of the Center for Collective Use «Molecular Biology» at the Institute of Biology of the Komi Scientific Centre of the Ural Branch RAS. The work was financially supported by the Ministry of Science and Higher Education of the Russian Federation State Assignment No. 125020301261-5 in the Institute of Chemistry of the Federal Research Center "Komi Scientific Centre", Ural Branch of the Russian Academy of Sciences and State Assignment No. 125020501526-3 in the Institute of Biology of the Federal Research Center "Komi Scientific Centre", Ural Branch of the Russian Academy of Sciences.

Author contribution. Pylina Y.I.: Writing – original draft; Writing – review and editing; Validation; Investigation; Formal analysis. Rocheva T.K.: Writing – original draft; Investigation; Formal analysis. Khudiaeva I.S.: Writing – original draft; Investigation; Formal analysis. Belykh E.S.: Conceptualization; Writing – original draft; Writing – review and editing; Investigation; Formal analysis. Shadrin D.M.: Writing – original draft; Writing – review and editing; Investigation; Formal analysis. Belykh N.D.: Investigation; Formal analysis. Belykh D.V.: Conceptualization; Supervision; Writing – original draft; Writing – review and editing

References

1. Abrahamse H., Hamblin M.R. *Biochem. J.* **2016**, *473*(4), 347–364. doi: 10.1042/BJ20150942.
2. Bryden F., Boyle R.W. *Metalloporphyrins for Medical Imaging Applications. In Advances in Inorganic Chemistry*. Amsterdam: Elsevier, **2016**. p. 141–221. doi: 10.1016/bs.adioch.2015.09.003.
3. Kwiatkowski S., Knap B., Przystupski D., Saczko J., Kędzierska E., Knap-Czop K., Kotlińska J., Michel O., Kotowski K., Kulbacka J. *Biomed. Pharmacother.* **2018**, *106*, 1098–1107. doi: 10.1016/j.biopha.2018.07.049.
4. Tsolekile N., Nelana S., Oluwafemi O.S. *Molecules* **2019**, *24*, 2669. doi:10.3390/molecules24142669.
5. Gunaydin G., Gedik M.E., Ayan S. *Frontiers in Chemistry* **2021**, *9*, 686303. doi: 10.3389/fchem.2021.686303.
6. Gunaydin G., Gedik M.E., Ayan S. *Frontiers in Chemistry* **2021**, *9*, 691697. doi: 10.3389/fchem.2021.691697.
7. Detty M.R., Gibson S.L., Wagner S.J. *J. Med. Chem.* **2004**, *47*(16), 3897–3915. doi: 10.1021/jm040074b.
8. Uchoa A.F., Oliveira C.S., Baptista M.S. *J. Porphyrins Phthalocyanines* **2010**, *14*, 832–845. doi: 10.1142/S1088424 61000263X.
9. Homayoni H., Jiang K., Zou X., Hossu M., Rashidi L.H., Chen W. *Photodiagnosis Photodyn. Ther.* **2015**, *12*, 258–266. doi: 10.1016/j.pdpdt.2015.01.003.
10. Fidanzi-Dugas C., Liagre B., Chemin G., Perraud A., Carrion C., Couquet C.-Y., Granet R., Sol V., Léger D.Y. *Biochimica et Biophysica Acta* **2017**, *1861*, 1676–1690. doi: 10.1016/ j.bbagen. 2017.02.003.
11. Dadeko A.V., Lilge L., Kaspler P., Murav'eva T.D., Starodubtcev A.M., Kiselev V.M., Zarubaev V.V., Ponomarev G.V. *Photodiagnosis Photodyn. Ther.* **2018**, *25*, 35–42. doi: 10.1016/j.pdpdt.2018.11.006.
12. Basoglu H., Degirmencioglu I., Eyupoglu F.C. *Photodiagn. Photodyn. Ther.* **2021**, *36*, 102615. doi: 10.1016/j.pdpdt. 2021.102615.
13. Ntoutoume G.M.A.N., Granet R., Mbakidi J.-P., Constantin E., Bretin L., L´eger D.Y., Liagre B., Chaleix V., Br´egier F., Sol V. *Bioorg. Med. Chem. Lett.* **2021**, *41*, 128024. doi: 10.1016/ j.bmcl.2021.128024.
14. Imran M., Ramzan M., Qureshi A.K., Khan M.A., Tariq M. *Biosensors* **2018**, *8*(4), 95. doi: 10.3390/bios8040095.
15. Diaz-Uribe C., Rangel D., Vallejo W., Valle R., Hidago-Rosa Y., Zarate X., Schott E. *Biometals* **2023**, *36*(6), 1257–1272. doi: 10.1007/s10534-023-00514-9.
16. Espitia-Almeida F., Díaz-Uribe C., Vallejo W., Gómez-Camargo D., Bohórquez A.R.R. *Molecules* **2020**, *25*(8), 1887. doi: 10.3390/molecules25081887.
17. Milanesio M.E., Alvarez M.G., Yslas E.I., Borsarelli C.D., Silber J.J., Rivarola V., Durantini E.N. *Photochem. Photobiol.* **2001**, *74*(1), 14–21. doi: 10.1562/0031-8655 (2001)0740014psomtm 2.0.co2.
18. Pavani C., Uchoa A., Oliveira C.S., Iamamoto Y., Baptista M.S. *Photochem. Photobiol. Sci.* **2009**, *8*, 233–240. doi: 10.1039/B810313E.
19. Malina L., Tomankova K.B., Malohlava J., Jiravova J., Manisova B., Zapletalova J., Kolarova H. **2016**, *34*, 246–256. doi: 10.1016/j.tiv.2016.04.010.
20. Sathisha M.P., Budagumpi S., Kulkarni N.V., Kurdekar G.S., Revankar V.K., Pai K.S.R. *Eur. J. Med. Chem.* **2010**, *45*, 106–113. doi: 10.1016/j.ejmech.2009.09.031.
21. Raman N., Jeyamurugan R., Senthilkumar R., Rajkapoor B., Franzblau S.G. *Eur. J. Med. Chem.* **2010**, *45*, 5438–5451. doi: 10.1016/j.ejmech.2010.09.004.
22. Qin J.-L., Shen W.-Y., Chen Z.-F., Zhao L.-F., Qin Q.-P., Yu Y.-C., Liang H. *Scientific Reports* **2017**, *7*, 46056. doi: 10.1038/srep46056.
23. Porchia M., Pellei M., Del Bello F., Santini C. *Molecules* **2020**, *25*, 5814. doi: 10.3390/molecules25245814.
24. Pellei M., Del Bello F., Porchia M., Santini C. *Coord. Chem. Rev.* **2021**, *445*, 214088. doi: 10.1016/j.ccr.2021.214088.
25. Rocheva T.K., Belykh D.V. *Russ. Chem. Bull.* **2023**, *72*, 1612–1617. doi: 10.1007/s11172-023-3941-8.
26. Lindhagen E., Nygren P., Larsson R. *Nat Protoc*. **2008**, *3*, 1364–1369. doi: 10.1038/nprot.2008.114.

27. Ritz C., Baty F., Streibig J.C., Gerhard D. *PLoS ONE* **2015**, *10*, e0146021. doi: 10.1371/journal.pone.0146021.
28. R Core Team (**2021**). R: A language and environment for statistical computing. R Foundation for Statistical Computing, Vienna, Austria. https://www.R-project.org/ (accessed 05.04.2025).
29. Pylina Y.I., Shadrin D.M., Shevchenko O.G., Startseva O.M., Velegzhaninov I.O., Belykh D.V., Velegzhaninov I.O. *Int. J. Mol. Sci.* **2017**, *18*, 103–116. doi: 10.3390/ijms18010103.
30. Selvin T., Berglund M., Lenhammar L., Lindskog M., Jarvius M., Larsson R., Nygren P., Fryknäs M., Andersson C.R. *BMC Pharmacology and Toxicology* **2024**, *25*, 25. doi: 10.1186/ s40360-024-00746-6.
31. Karlsson H., Fryknäs M., Senkowski W., Larsson R., Nygren P. *Oncology Letters* **2022**, *23*, 123. doi: 10.3892/ ol.2022.13243.
32. Belykh D.V., Kozlov A.S., Pylina Y.I., Khudyaeva I.S., Benditkis A.S., Krasnovsky A.A. *Macroheterocycles* **2019**, *12*, 68–74. doi: 10.6060/mhc190128b.
33. Startseva O.M., Pylina Y.I., Shadrin D.M., Belykh E.S., Shevchenko O.G., Velegzhaninov I.O., Belykh D.V. *J. Porphyrins Phthalocyanines* **2022**, *26*, 91–103. doi: 10.1142/ S1088424621500899.
34. Berezin D.B., Kruchin S.O., Kukushkina N.V., Venediktov E.A., Koifman M.O., Kustov A.V. *Photochem.* **2023**, *3(1)*, 171–186. doi: 10.3390/photochem3010011
35. Kustov A.V., Krestyaninov M.A., Kruchin S.O., Shukhto O.V., Kustova T.V., Belykh D.V., Khudaeva I.S., Koifman M.O., Razgovorov P.V., Berezin D.B. *Mendeleev. Commun.* **2021**, *31(1)*, 65–67. doi: 10.1016/j.mencom.2021.01.019
36. Kustov A.V., Privalov O.A., Strelnikov A.I., Koifman O.I., Lubimtsev A.V., Morshnev P.K., Moryganova T.M., Kustova T.V., Berezin D.B. *J. Clin. Med.* **2022**, *11*, 233. doi: 10.3390/ jcm11010233.
37. Kustov A.V. *ChemChemTech [Izv. Vyssh. Uchebn. Zaved. Khim. Khim. Tekhnol.]* **2023**, *66*(12), 32–40. doi: 10.6060/ ivkkt.20236612.6902.
38. Kustov A.V., Morshnev F.K., Shukhto O.V., Smirnova N.L., Kukushkina N.V., Koifman O.I., Berezina D.B. *Russ. Chem. Bull.* **2023**, *72*, 566–573. doi: 10.1007/s11172-023-3820-2.
39. Kustov A.V., Morshnev Ph.K., Kukushkina N.V., Smirnova N.L., Berezin D.B., Karimov D.R., Shukhto O.V., Kustova T.V., Belykh D.V., Mal`shakova M.V., Zorin V.P., Zorina T.E. *Int. J. Mol. Sci.* **2022**, *23*, 5294. doi: 10.3390/ijms 23105294.
40. Shukhto O.V., Khudyaeva I.S., Belykh D.V., Berezin D.B. *ChemChemTech* [*Izv. Vyssh. Uchebn. Zaved. Khim. Khim. Tekhnol.*] **2021**, *64*(11), 86–96. doi: 10.6060/ivkkt.20216411. 6500.
41. Zhang X.-H., Zhang L.-J., Sun J.-J., Yan Y.-J., Zhang L.-X., Chen N., Chen Z.-L. *Biomed. Pharmacother.* **2016**, *81*, 265–272. doi: 10.1016/j.biopha.2016.04.007.
42. Nishie H., Kataoka H., Yano Sh., Yamaguchi H., Nomoto A., Tanaka M., Kato A., Shimura T., Mizoshita T., Kubota E., Tanida S., Joh T. *Biochem. Biophys. Res. Commun.* **2018**, *496*(4), 1204–1209. doi: 10.1016/j.bbrc.2018.01.171.
43. Belykh D.V., Pylina Y.I., Kustov A.V., Startseva O.M., Belykh E.S., Smirnova N.L., Shukhto O.V., Berezin D.B. *Photochem. Photobiol. Sci.* **2024**, *23*, 409–420. doi: 10.1007/s43630-023-00527-w.
44. Pylina Y.I., Khudiaeva I.S., Belykh D.V. *Macroheterocycles* **2022**, *15*, 25–33. doi: 10.6060/mhc224176b.
45. Sengupta D., Timilsina U., Mazumder Z.H., Mukherjee A., Ghimire D., Markandey M., Upadhyaya K., Sharma D., Mishra N., Jha T., Basu S., Gaur R. *Eur. J. Med. Chem.* **2019**, *15*(74), 66–75. doi: 10.1016/j.ejmech.2019.04.051.
46. Ježek J., Cooper K.F., Strich R. *Antioxidants* **2018**, *7*, 13. doi: 10.3390/antiox7010013.
47. Villalpando-Rodriguez G.E., Gibson S.B. *Oxid. Med. Cell. Longev.* **2021**. 9912436. doi: 10.1155/2021/9912436.
48. Liu L., An X., Schaefer M., Yan B., de la Torre C., Hillmer S., Gladkich J., Herr I. *Biomed. Pharmacother.* **2022**, *153*, 113511. doi: 10.1016/j.biopha.2023.115879
49. Shlomovitz I., Speir M., Gerlic M. *Cell Commun. Signal.* **2019**, *17*, 139. doi.: 10.1186/s12964-019-0437-0.
50. Furuta Y., Zhou Z. *Front. Cell Dev. Biol.* **2023**, *11*, 1170551. doi: 10.3389/fcell.2023.1170551.
51. Legrand A.J., Konstantinou M., Goode E.F., Meier P. *Molecular Cell* **2019**, *76*, 232–242. doi: 10.1016/j.molcel. 2019.09.006.
52. Rehfeldt S.C.H., Laufer S., Goettert M.I. *Int. J.Mol. Sci.* **2021**, *22*, 3701. doi: 10.3390/ijms22073701.
53. Zaib S., Hayyat A., Ali N., Gul A., Naveed M., Khan I. *Anti-Cancer Agents Med. Chem.* **2022**, *22*, 2048–2062. doi: 10.2174/1871520621666211126090906.
54. Gomes M.T., Palasiewicz K., Gadiyar V., Lahey K., Calianese D., Birge R.B., Ucker D.S. *J. Biol. Chem.* **2022**, *298*(7), 102034. doi: 10.1016/j.jbc.2022.102034.

Received 02.03.2025
Accepted 05.04.2025